JOURNAL OF MECHANICAL ENGINEERING AND SCIENCES
ISSN: 2289-4659 e-ISSN: 2231-8380
VOLUME 19, ISSUE 3, 2025, 10791 - 10804
DOI: https://doi.org/10.15282/jmes.19.3.2025.8.0846

RESEARCH ARTICLE

Optimization of exoskeleton design for post-stroke ankle rehabilitation based on kinematic and structural model evaluation

Eko Wahyu Abryandoko*, Faisal Ashari

Department of Industrial Engineering, Universitas Bojonegoro, 62115, Bojonegoro, Indonesia
Phone: +62 85645279821

ABSTRACT - Ankle rehabilitation is a crucial indicator of walking ability recovery, as it serves as a marker of early mobility function recovery in post-stroke patients. Robot-assisted ankle rehabilitation is more effective in restoring range of motion, balance, and gait proprioception in patients with ankle injuries. This study aims to optimize the design of an ankle rehabilitation exoskeleton through structural simulation, biomechanical alignment, and efficiency based on several alternative actuator designs. Alternative exoskeleton designs focus on the rehabilitation of dorsiflexion-plantarflexion and inversion-eversion movements. The analysis method for assessing the best exoskeleton design alternatives uses an engineering design methodology approach based on static and dynamic test parameters, namely kinematics and finite element analysis. The results of the design engineering implementation show that the exoskeleton design with Concept B is more efficient based on several mechanical test parameters compared to Concept A. Simulation results show that Design B alternative is superior in all test parameters with a value of (4.22 versus 3.68) in the safety factor, a lower peak stress of (30.43 MPa versus 39.15 MPa), and produces energy efficiency with lower torque requirements. The mechanical stability of Concept B is characterized by utilizing a more efficient actuator design with enhanced safety features for users. Based on the parameters and characteristics of the simulation test using design engineering, Design B is more feasible for development as a robotic mechanical system to meet the needs of post-stroke patient ankle rehabilitation.

ARTICLE HISTORY
Received : 26th Dec. 2024
Revised : 06th June 2025
Accepted : 09th Sept. 2025
Published : 30th Sept. 2025

KEYWORDS
Exoskeleton design engineering
Simulation
Ankle
Stroke rehabilitation

1. INTRODUCTION

The 2019 Global Burden of Disease (GBD) estimates show that stroke is the second leading cause of death and the third leading cause of disability (expressed in terms of years of life lost due to disability, Disability-Adjusted Life Years) worldwide [1]. The World Health Organization (WHO) reports that more than 15 million people are affected by stroke each year, projected to increase to 3.4 million cases per year by 2030 [3, 4]. One important indicator of recovery in stroke patients is the ability to walk, because the range of motion of the leg is used by medical personnel as a marker of early recovery of patient mobility function [4]. The ankle joint range of motion is the third important factor that can affect a patient's ability to walk, after spasticity and muscle strength [5]. According to Bourgeois et al. [6]. Ankle rehabilitation is a crucial factor in strengthening balance muscles and improving proprioception, which is essential for regaining the ability to walk in patients with post-stroke conditions. Recently, the use of a robotic system in post-stroke patient recovery efforts has shown intensity, consistency, and progress tracking compared to conventional rehabilitation [8, 9]. One of the assistive technologies that can provide controlled repetitive movements in rehabilitation programs is the lower limb exoskeleton.

Numerous studies have identified lower limb exoskeletons as promising assistive devices for facilitating the rehabilitation of the ankle joint. [9, 10]. However, the development of exoskeletons still faces challenges in human-robot interaction, particularly in designing actuator mechanisms with optimal energy efficiency, which is crucial for their sustainable and safe use in rehabilitation processes. Suboptimal exoskeleton actuator mechanism design can result in reduced responsiveness to user needs, leading to collisions between robot systems [11, 12]. According to Barkataki et al. [13], the active and comfortable assistance during rehabilitation using exoskeletons is greatly influenced by the design of mechanisms that align with the user's anthropomorphic characteristics. A growing body of literature has been dedicated to the development and refinement of lower limb exoskeleton systems in recent years. A four-degree-of-freedom (DOF) passive lower limb exoskeleton was developed by Gonçalves et al. [14], who proposed biomechanical principles and optimized it through a differential evolution-type genetic algorithm within a mathematical modeling framework. The study by Umesh et al. [18] employed continuum posture analysis to assess the pressure distribution on the exoskeleton structure under the patient's body weight during sit-to-stand transitions. Narayan et al. [15] developed a sliding rail mechanism model for the thigh and calf, with a limited height adjustment range, based on the proportion of children's legs, utilizing the design of a lower limb exoskeleton system (Lower Limb Exoskeleton, LLE). On the other hand, research by Collins et al. [16]. Developed a passive ankle exoskeleton that reduced the metabolic cost of walking by up to 7.2% without additional energy input. However, the use of responsive actuators with optimal energy efficiency remains a

*CORRESPONDING AUTHOR | E. W. Abryandoko | ✉ abryandoko@gmail.com

challenge, particularly in positioning patients correctly and comfortably during ankle motor rehabilitation. Optimization of actuator design is crucial for developing an effective exoskeleton model that facilitates ankle joint recovery in post-stroke patients.

To achieve an optimal exoskeleton configuration, this study employs a comprehensive engineering design methodology as the foundation for design development. [17]. The criteria for assessing design performance are determined based on finite element analysis (FEA) simulation parameters and motion analysis. The primary focus of this study is to analyze the physiology, biomechanics, and pathology of the ankle, establishing design criteria based on the required range of motion of the ankle joint, specifically in dorsiflexion-plantarflexion and inversion-eversion. Second, static and dynamic simulation tests were conducted using motion analysis and FEA, based on kinematic parameters and ankle segment weight configurations. Testing is performed to determine the optimal design alternative through various assessment parameters, including torque value, von Mises stress evaluation, displacement, and safety factor. Third, alternative exoskeleton designs are analyzed by comparing convolutional matrices to determine the best design solution based on the predetermined performance criteria. The application of the engineering design methodology is expected to produce an energy-efficient exoskeleton design that meets the requirements for ankle rehabilitation in post-stroke patients.

1.1 Study of Anatomy, Physiology, and Biomechanical Aspects

As a basis for designing the exoskeleton, an anatomical study was conducted using an ankle biomechanical system approach. This study aimed to rehabilitate the ankle by increasing its range of motion through functional movements of plantar flexion, dorsiflexion, eversion, and inversion. The biomechanical structure of the ankle serves as an essential joint connecting the lower leg and foot, formed by the fusion of the talus, fibula, and tibia bones, which allows for flexion-related movements [21, 22]. The downward motion of the foot is produced by plantar flexion, while dorsiflexion causes the toes to lift off the ground. Additionally, limited movements, including pronation, supination, inversion, and eversion, play essential roles in enhancing both the flexibility and steadiness of the foot. Plantar flexion and dorsiflexion movements are controlled by the sagittal plane of the ankle, while abduction and adduction are coordinated through the transverse plane. On the other hand, inversion and eversion movements are controlled in the frontal plane. Anatomical differences, cultural and geographic influences, and variations in angle measurement techniques often shape individual differences in ankle range of motion. Figure 1 illustrates the primary motions of the ankle that serve as a foundational reference in designing the exoskeleton's mechanical structure [20]. The mechanical structure of the exoskeleton was developed using ankle joint motion. Figure 1 explains the design constraints. Motions include plantar flexion (≤ 45°), dorsiflexion (0°–20°), inversion (≤ 30°), and eversion (≤ 20°) [21]. Anatomical and mechanical analogies based on ankle motion characteristics serve as the basis for the exoskeleton design. The robotic joint system is required to replicate the ankle range of motion (ROM) and maintain alignment with the natural joint during all biomechanical activities [26, 27].

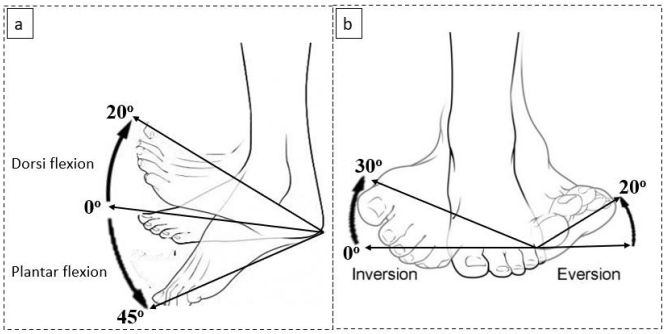

Figure 1. Illustrates the ankle joint movements incorporated into the exoskeleton's kinematic design: (a) dorsiflexion–plantarflexion and (b) inversion–eversion

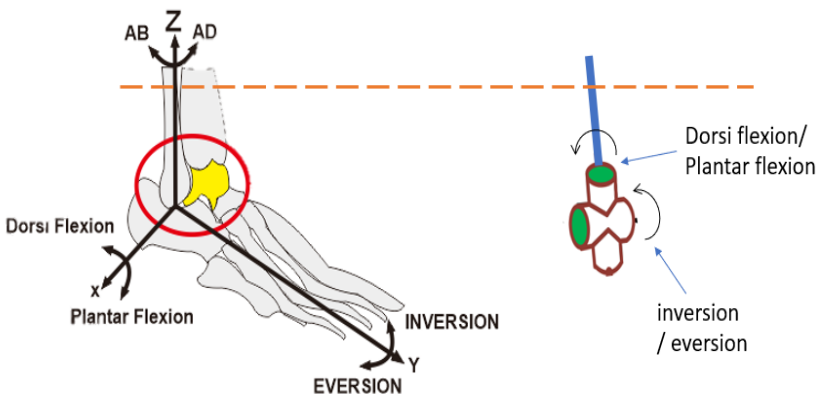

Figure 2. Functional correlation between ankle movement and anatomical-mechanical design framework [22]

1.2 Design Criteria and Requirements for Exoskeleton Systems

The exoskeleton configuration is anatomically designed to support a wide range of patients, taking into account differences in height, weight, and age demographics. To optimize comfort during use, the outer frame design takes into account anthropometric data, such as the dimensions and weight distribution of the ankle segment. Ankle length measurements were based on anthropometric data specifically for the Indonesian population [25], while segmental leg weight was calculated by referring to the proportion of ankle segment mass distribution [26], as described in Table 1.

Table 1. Anthropometric dimensions and weight distribution of lower limb segments

Leg Segment	5th Percentile (cm)	50th Percentile (cm)	95th Percentile (cm)	Weight Distribution (% of body mass)
Foot Length (sole)	14.59	22.73	30.87	—
Knee Height	36.16	48.12	60.08	9.3%
Foot Width (sole)	6.29	9.14	11.98	2.9%

To assess the mechanical load capacity of the exoskeleton, the mass of the forearm and hand was estimated. These values were calculated based on the assumption that the body weight in this study was a maximum of 75 kg, so the calculation is as follows [25]:

$$\text{Knee Height Segment Weight} = \frac{75\ kg \times 9.3\%}{2} = 3.48\ kg$$

$$\text{Weight of Pair Foot Segment} = \frac{75\ kg \times 2.9\%}{2} = 1.08\ kg$$

$$\text{Total Weight of One Leg Segment} = 3.48\ kg + 1.08\ kg = 4.56\ kg$$

The weight of a single leg segment, assuming a body weight of 75 kg, is 4.56 kg, which is the combined height of the knee and the sole of the foot. Leg segment weight calculations are entered as input parameters in the simulation process to assess the exoskeleton mechanism. Additional design factors used include ensuring patient safety and comfort when the exoskeleton is operated within normal working ranges of motion and speeds. Human ankle range of motion evaluation is also performed to accommodate patient safety and comfort requirements during device use [26]. The exoskeleton movement mechanism design must remain within a range smaller than the patient's ankle dorsiflexion–plantarflexion and inversion–eversion capabilities while the device is in operation. A comparison of the ankle and device motion parameter ranges is outlined in Table 2 [32, 33]. The motion configuration of the exoskeleton is tailored to the ankle's normal range of motion, ensuring patient comfort and safety due to its function as a primary load-bearing mechanism. To avoid exceeding normal joint function, the design incorporates motion limitations for plantar and dorsiflexion, as well as inversion-eversion, which helps prevent injury and maintain patient comfort during use.

Table 2. Comparison of ankle and device motion parameter ranges

Types of Motion	Anatomical Range	Proposed Device Range
Plantar flexion	45°	40°
Dorsi flexion	20°	15°
Eversion	20°	10°
Inversion	30°	30°

Table 3. Simulation test categories for exoskeleton structure design

Simulation Category	Purpose of Simulation	References
Kinematic Simulation	Simulate the angular velocity trajectory of exoskeleton movement	[36, 37]
Finite Element Method	Examination of structural performance involving nodal force application, resulting displacements, and safety assessment parameters.	[38, 39]
Torsional Load Simulation	Assesses torsional stress in ankle-related movements: Plantarflexion, dorsiflexion, inversion, and eversion.	[40, 41]

1.3 Mechanical Framework Design of the Exoskeleton

A systematic framework incorporating the Pugh decision matrix is used in designing exoskeleton structures to compare several alternative designs [34, 35]. To examine stresses and deformations in CAD designs, the identification process utilizes finite element analysis (FEA) simulation techniques. To select the best-performing outer frame design in terms of material and structure, several simulation-based evaluations were performed, as summarized in Table 3. To determine the optimal design, simulation test results are systematically compared using a decision matrix. This systematic

approach relies on predefined benchmarks to select the most appropriate design. Figure 3 shows the criteria used to develop the ankle rehabilitation exoskeleton.

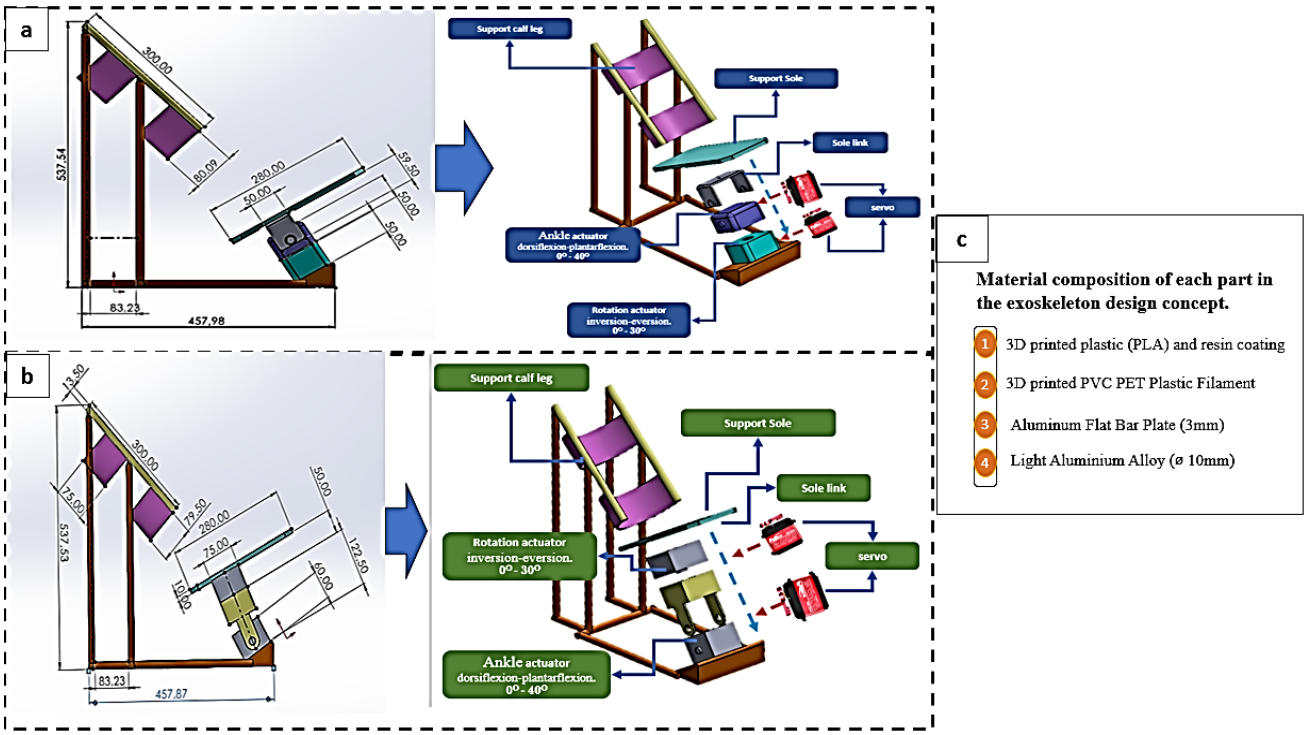

Figure 3. Illustrates the Structural Configuration of the Ankle Rehabilitation Exoskeleton: (a) Design of direct actuator integration with the joint, (b) design of mechanical structure incorporating extended lever arms and connectors, and (c) design of material composition selected for the exoskeleton

Figure 3 shows two 2-DOF exoskeleton mechanisms as part of a rehabilitation framework designed to facilitate ankle dorsiflexion–plantarflexion and inversion–eversion movements. The alternative exoskeleton designs differ in the actuator structure to support the lower leg and sole of the foot. As shown in Figure 3(a), direct coupling of the actuator to the joint is used to create a compact structure with minimal mechanical components and short joints. Meanwhile, the configuration in Figure 3(b) uses an additional connection via a longer lever, which provides more balanced mechanical forces and reduces stress concentrations, supporting the long-term stability of the device. Both alternatives are designed to follow the patient's natural joint motion, although defining an effective coupling mechanism between the actuator and the human joint remains a significant design challenge. Cempini et al. [37] emphasized that improper coupling alignment can cause discomfort or injury. In line with this, to enhance ergonomic design and user adaptability, Celebi et al. [43] recommended employing a Schmidt coupling system actuated by SEAs. In parallel, Erdogan et al. [44] reported that parallel mechanisms facilitate accurate limb alignment during movement. However, to ensure safe interaction, joint kinematics and physiological limits must be taken into account to prevent misalignment or overextension [45, 46]. Optimizing the design of the exoskeleton is crucial, as the compact actuator layout facilitates balanced force transmission, thereby enhancing comfort, safety, and stability during ankle rehabilitation movements.

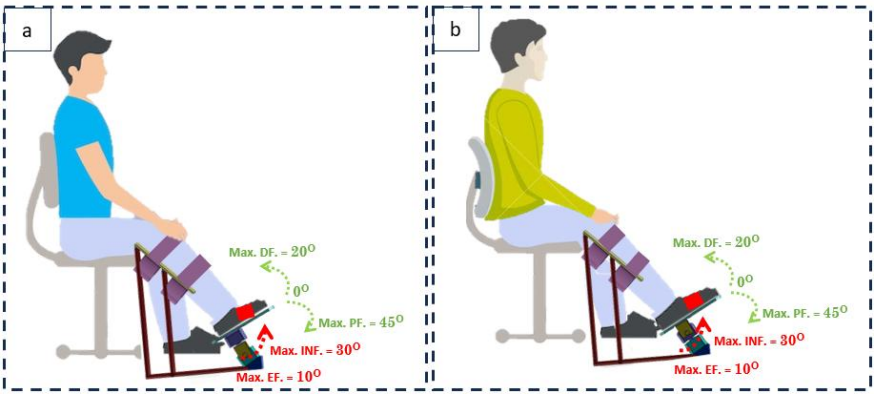

Figure 4. Conceptual design of the exoskeleton and placement of the actuators relative to the ankle joint: (a) Concept design configuration showing the rotation mechanism connected directly to the joint structure, and (b) Concept design configuration showing the rotation mechanism acting as a structural support for the joint.

The materials used for the ankle exoskeleton were selected to meet the simulation objectives and enable coordinated motion performance. This design integrates a footplate mounted on the user's foot and a stiff upper frame connected to the lower limb for structural support. Pivot joints enable rotational motion in the sagittal plane, thereby supporting the natural motion of the ankle. Structural simulation validates load resistance, while FEA determines mechanical stresses, deformation rates, and safety factors. Motion analysis is simulated in SolidWorks 2022a to ensure the operational feasibility of the design under predefined conditions. Efficiency in rehabilitation technology refers to the safe and effective completion of rehabilitation movements [47, 48]. The exoskeleton structure must be able to support postural stability and resistance to external forces to provide a safe rehabilitation context [49, 50]. Figure 4 shows the actuator placement and structural design of the ankle joint exoskeleton. The proposed alternative exoskeleton design encompasses the entire range of motion, tailored to the physiology of the ankle. The exoskeleton design moves within a limiting angle determined by calculating the length and weight of the ankle segment. Spatial specifications are maintained by considering adaptation to various anthropometric proportions of individuals, thereby preventing collisions with the robotic system when switching configurations between subjects. All planned parameters, such as range of motion and leg segment loads, are calculated to obtain optimal FEA simulation test results and torsional strength, enabling the exoskeleton to be analyzed for safety, efficiency, smooth movement, and structural stability within the patient's workspace during surgery.

2. MATERIAL AND METHODS

This research employed a systematic approach to develop and evaluate an exoskeleton designed for post-stroke lower limb therapy. The complete sequence of steps is depicted in Figure 5.

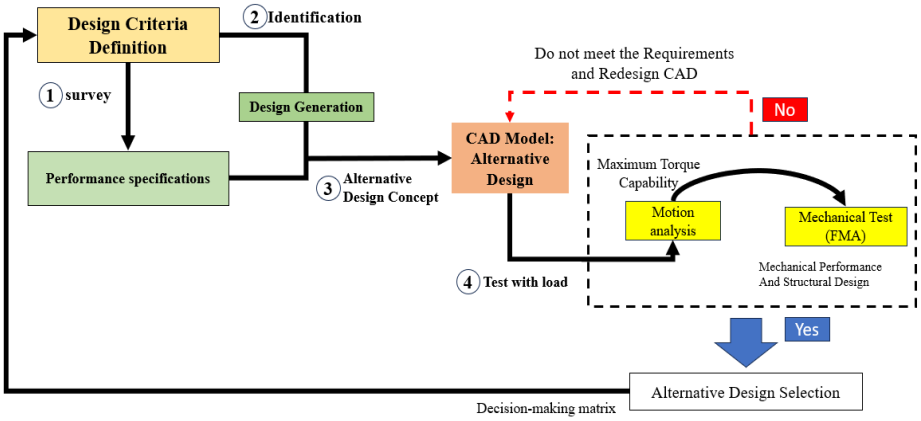

Figure 5. Systematic workflow for alternative exoskeleton design selection based on mechanical and motion analysis

2.1 Design Parameterization using Computer-Aided Modeling Tools

The exoskeleton design was formed in three dimensions using SolidWorks to represent detailed and realistic CAD modeling. CAD modeling and simulation analysis were performed to determine the parameters for motion testing and structural analysis. The developed design alternatives were determined based on the anthropometry of the ankle and lower leg in adults. The length parameters of the leading leg structure segment were used to determine the position of the connecting rod and the location of the actuator. The main leg structure segment parameters were used to ensure optimal alignment between the structure and function of the exoskeleton. The inclusion criteria for the CAD modeling process are described as follows:

a) Anthropometric approach: The exoskeleton design criteria are adjusted to the dimensions and angles of the ankle. The height range used as a reference is 160–175 cm with a foot length of 24–26 cm. The physiological movement of the ankle joint is determined by the range of motion, based on normal movement, which includes 40° of dorsiflexion and plantarflexion, and 30° of inversion and eversion.

b) Actuator design: The alternative actuator designs for exoskeletons in designs A and B are assessed based on the influence of housing shape, connection points, and mechanical movement paths.

c) Materials: the exoskeleton structure is designed using materials such as PLA and PET (3D printing), and the frame structure uses a combination of flat and lightweight aluminum

d) Structural Boundary Parameters: The exoskeleton design was simulated with the parameters of the frame base plate area and the grounding conditions. The actuator joint was subjected to a load of 44.7 N (equivalent to 4.47 kg) to analyze the gravitational force at the loading point during the ankle rehabilitation process.

e) Mesh generation: Meshing techniques in SolidWorks Simulation are used to determine the Global Element Size and Tolerance values. The standard mesh determination is adjusted to discretize the model into tetrahedral elements, allowing for optimal estimation of high stress concentrations at the actuator joints and frame joints.

f) Simulation integration: The assembly of the CAD model is simulated based on static structural parameters and corresponding loads. The simulation results of the alternative exoskeleton CAD model are evaluated, including von Mises stress, displacement, and safety factor. Additionally, kinematic modeling is performed using motion analysis to determine the magnitude of the estimated torque generated by the two alternative exoskeleton designs.

The modeling process using this CAD model serves as a visual and technical basis for systematically determining the best design criteria using a matrix.

2.2 Design Evaluation and Selection

Exoskeleton design alternatives are determined based on the most optimal CAD model simulation criteria using the Pugh decision matrix [6]. Multicriteria decision-making is assessed using five main evaluation criteria. Criteria weight refers to the relative importance of the preferred direction of post-stroke ankle rehabilitation. The inclusion criteria for exoskeleton design alternatives are presented in Table 4. Table 4 outlines several key inclusion criteria for determining the optimal exoskeleton design. Each weight is determined based on the importance of the exoskeleton mechanism performance for the needs of ankle rehabilitation in post-stroke patients. Determination of the dorsiflexion-plantarflexion torque weight (30%) and inversion-eversion torque (25%) because the movement has a direct impact on the selection of actuators and energy efficiency, thus minimizing actuator torque without sacrificing functionality. The evaluation assigned a 25% weighting to the safety factor, indicating a direct impact on structural strength and patient safety. Displacement and tensile stress each received a 10% weighting, indicating their relevance in determining structural consistency and material durability. The assigned weights contribute to a more data-driven and clinically aligned decision-making process for post-stroke ankle rehabilitation exoskeletons.

Table 4. Evaluation criteria and weighting based on engineering design methodology

No.	Design Evaluation Criteria	Description of Design Criteria Evaluation	Preference Direction	Importance Factor
1	Motion analysis Dorsiflexion–Plantarflexion (N·m)	Torque for vertical movement to facilitate up-and-down ankle motion	Lower is better	30%
2	Motion analysis Inversion–Eversion (N·m)	Driving torque for side-to-side ankle movement	Lower is better	25%
3	Tensile Stress (MPa)	Determines structural strength under tensile load	Higher is better	10%
4	Displacement (mm)	Assesses structural deformation parameters	Lower is better	10%
5	Safety Factor	Evaluates the safety margin against structural failure	Higher is better	25%
	Total			100%

3. RESULTS AND DISCUSSION

3.1 CAD Model of the Kinematic Structure of the Robotic System

Kinematic analysis in the exoskeleton simulation workspace was conducted to evaluate the motion trajectory tracking capability of two alternative designs. The input motion values used were in the form of sinusoidal waves with a motion angle amplitude of 0°–40° for dorsiflexion–plantarflexion and 0°–30° for inversion–eversion [44]. The motion angle parameters represent the physiological limits of the ankle joint, allowing for the identification of the torque characteristics required for each design during the rehabilitative movement cycle. These characteristics are evaluated based on the dynamic response to changes in position, such as torque parameters, speed, and movement accuracy. The primary objective is to establish a technical foundation for designing an optimal energy-efficient system that responds to loads [52-54]. Visualization of motion analysis based on kinematics is shown in Figure 6. Figure 6 shows the motion trajectory of the exoskeleton design alternatives. This test aims to determine the optimal exoskeleton design for supporting ankle rehabilitation. The trajectory tracking simulation was conducted with a load adjusted to meet the subject's rehabilitation needs, evaluating the design's ability to control dorsiflexion–plantarflexion and inversion–eversion movements. Zhu et al. [48] stated that exoskeleton motion simulation is capable of predicting system models with controlled and precise motion replication at complex joint amplitudes. Safe and comfortable limits can be observed through accurate amplitude control of displacement, velocity, acceleration, and jerk during operation [56, 57]. Optimizing the workspace in the design is a significant concern, ensuring that the dimensions and positions of the exoskeleton components remain compact, so that the functional aspects of the exoskeleton do not hinder the user's natural movements during therapy [58, 59].

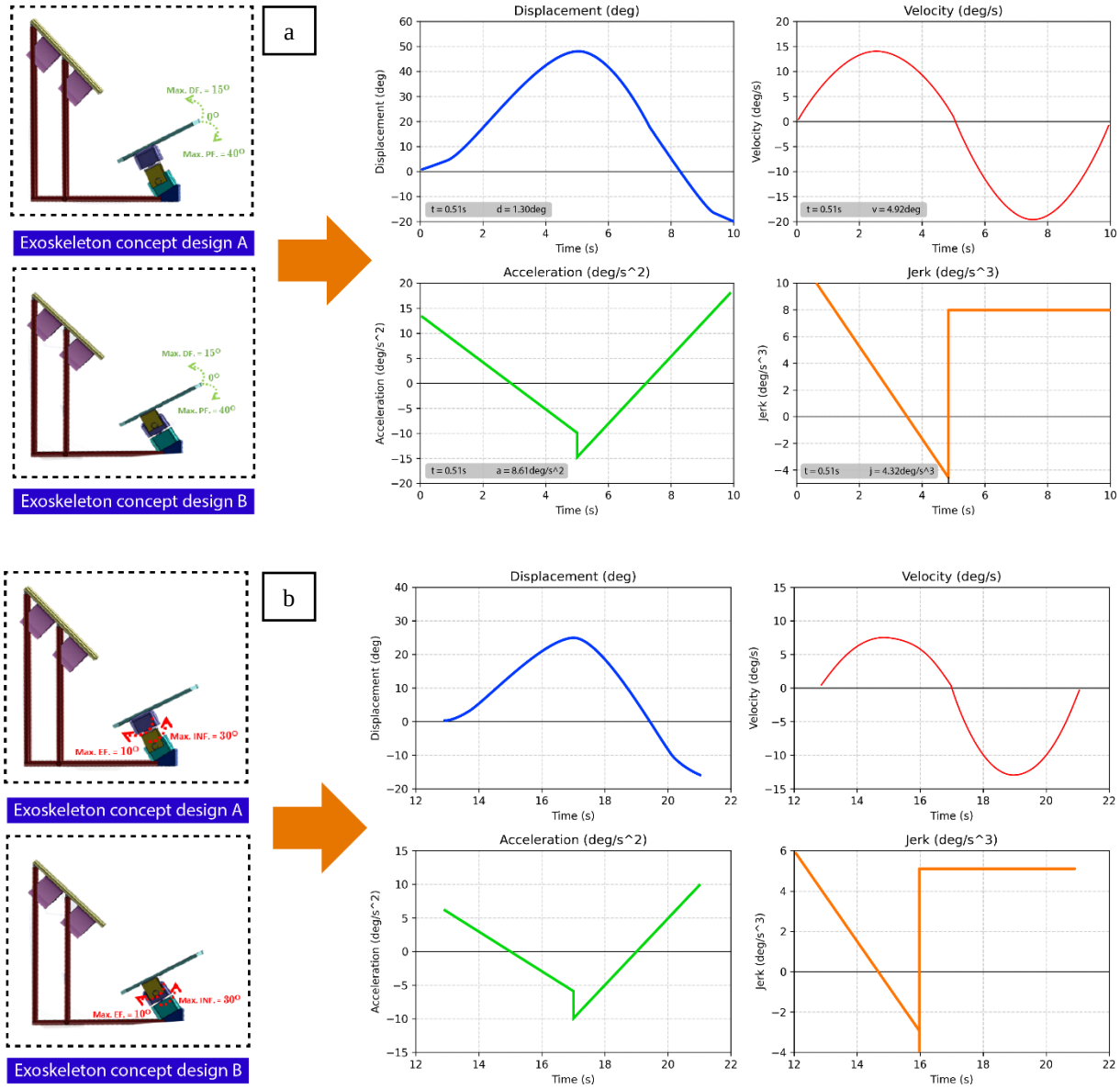

Figure 6. Angular trajectory tracking for dorsiflexion–plantarflexion and inversion–eversion motions on two alternative exoskeleton designs: (a) The rotational velocity profile of the dorsiflexion–plantarflexion angle is ω = 0,698 rad/s (40°/s) and (b) The rotational velocity profile of the dorsiflexion–plantarflexion angle is ω = 0.524 rad/s (30°/s)

3.2 Dynamic Motion Evaluation

The simulation of movement performance is assessed based on the exoskeleton's ability to lift loads and compensate for gravity, as demonstrated by a load of 44.73N, which is adjusted according to the total weight calculation in the Equation. A 50% load is added to each parameter to account for material variability, allowing for error values during prototyping. Additionally, the addition of the load aims to assess the exoskeleton's performance in response to a material change. The maximum torque estimate for each exoskeleton design criterion is used as a consideration in determining the actuator with more efficient energy consumption and in meeting the needs of post-stroke patient ankle rehabilitation. Figure 7 is the result of the torque simulation of each proposed exoskeleton criterion. Torque performance simulations generated from both exoskeleton design alternatives show significant differences, with design alternative B being lower than design A in each movement. The torque value from the dorsiflexion-plantar flexion motion simulation in design alternative B is 360 Nm, while design A reaches a peak torque of up to 842 Nm. The same results also occur in the inversion-eversion motion simulation of design alternative B (134 Nm vs. 170 Nm), which is lower than that of design alternative A. This difference indicates that different actuator design alternatives, even when subjected to the same load, can produce varying torque values. The results of the analysis show that design alternative B is more considered because it produces higher energy efficiency compared to design alternative A. This energy efficiency advantage can lead to more stable control performance in the use of post-stroke patient ankle rehabilitation. A comparison of torque value results is shown in Figure 9. The comparison of maximum torque values in Figure 9 illustrates the superior energy efficiency of alternative design B compared to design A. Alternative design A requires greater torque to drive the actuator during lifting

of the ankle load in dorsiflexion, plantar flexion, and inversion–eversion movements. In contrast, alternative design B is more energy-efficient, making it a better choice for applications that prioritize efficiency over maximum strength. The structural design configuration in alternative design B can distribute the load more evenly. The resulting energy efficiency enables system control with lighter and more responsive actuators. This is supported by the opinion of Mashud et al. [53], who stated that actuators with lower torque can produce a smoother movement control system, thereby increasing user comfort during repeated rehabilitation sessions. Simulation of the exoskeleton's movement characteristics reveals parameters that align with the patient's physiological limits [54].

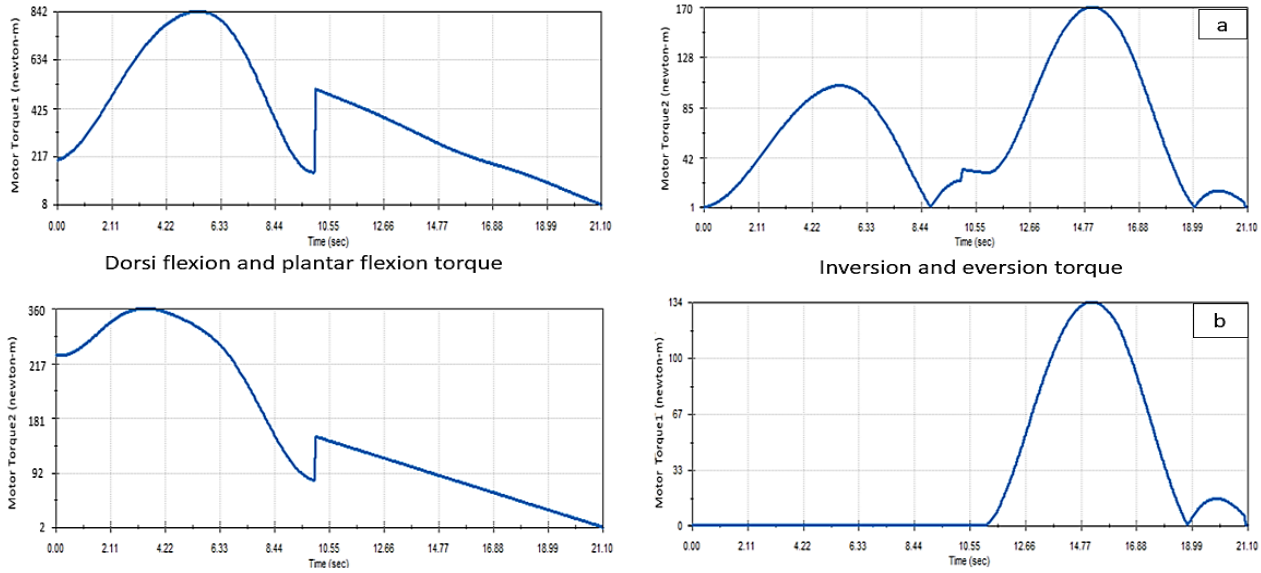

Figure 7. Maximum Torque Capacity of the Exoskeleton During Dorsiflexion–Plantarflexion and Inversion–Eversion Movements: (a) Torque performance of alternative exoskeleton design A and (b) Torque performance of alternative exoskeleton design B

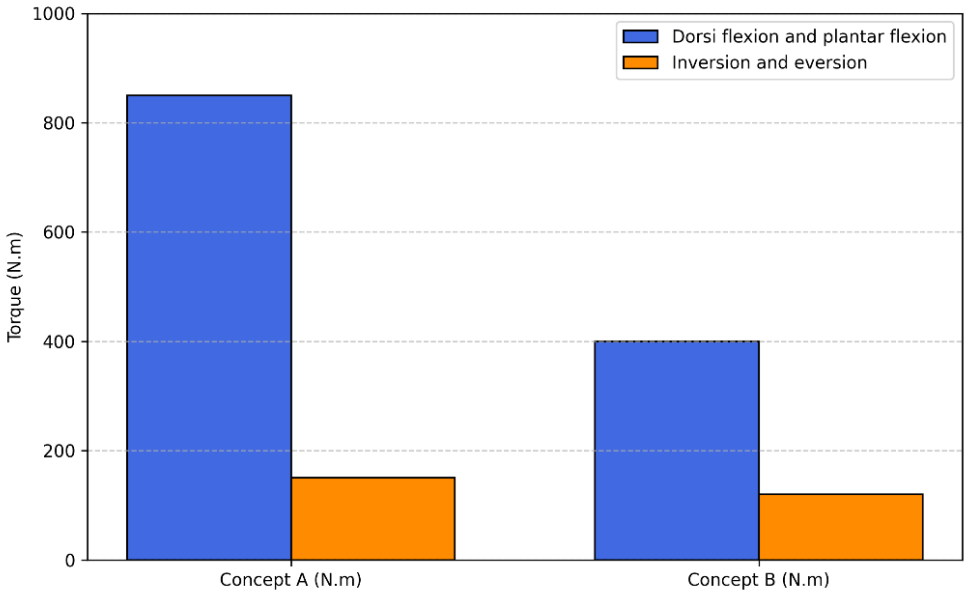

Figure 8. Recapitulation of torque moments between alternative design A and design B

3.3 Structural Performance Analysis with Finite Element Modeling

Analysis of the mechanical structure performance of the exoskeleton in performance testing based on FEA. The provision of operational loads is adjusted based on predetermined parameters. The evaluation of two alternative exoskeleton designs is assessed based on pressure distribution parameters, stress, and deformation levels to determine the structural strength, stability, and durability values of each design [63]. The critical stress patterns of the exoskeleton components are identified to determine the optimal design with the best safety and reliability criteria in supporting post-stroke patient ankle rehabilitation. FEA visualization of both designs is shown in Figures 9 and 10. FEA simulations on all aspects of the structural and mechanical performance of the outer frame indicate that Design B is superior to Design A. Design B produces maximum von Mises stress (30.43 MPa vs. 39.15 MPa), superior to Design A. The von Mises

stress in Design A is concentrated around the actuator mount and joints, indicating that the actuator mount area is susceptible to failure due to long-term use. In contrast, Design B produces a more even stress pattern, especially at the joints and actuators. Structural flexibility. The total displacement of both outer frame design alternatives remains within acceptable mechanical tolerances, with Design B (1.78 mm vs. 1.55 mm) being slightly higher than Design A. Critical load scenarios with design thresholds indicate that both outer frame design alternatives can provide a factor of safety with a structural reliability margin. Design B is able to produce 4.22 versus 3.68, with a higher structural reliability margin than Design A. Notably, both design alternatives are able to reduce the potential for local cracking or deformation.

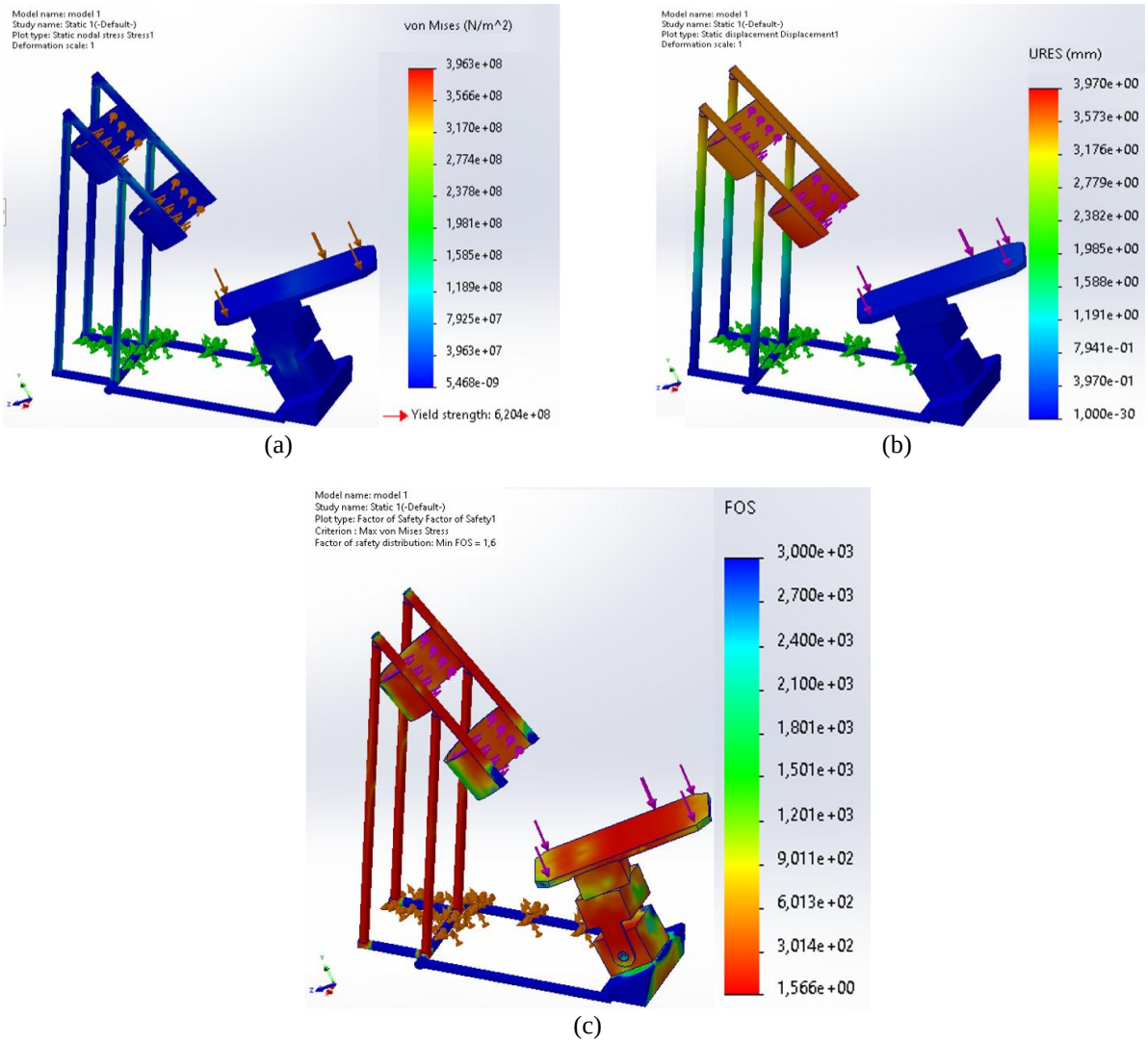

Figure 9. FEA simulation results on exoskeleton design alternative A: (a) Tension test, (b) Displacement test, and (c) Safety factor

3.4 Design Alternative Evaluation Matrix

The selection process for the two alternative designs is determined based on torque and FEA values; this stage is essential to ensure that the developed exoskeleton meets the expected specifications [64]. The decision matrix method is employed as an objective evaluation framework, utilizing specific actuator and mechanical structure criteria values, such as energy efficiency, reliability, and ease of operation, for the exoskeleton [65]. The systematic selection process for the two alternative exoskeleton designs is determined based on the technical needs of the ankle rehabilitation process for post-stroke patients. Table 5 presents the decision-making matrix with technical criteria weights from the results of the torque and FEA simulation analysis on two alternative exoskeleton designs. The technical criteria are determined based on the weights specified in Table 4. The weighting results in the decision-making matrix show that alternative design B outperforms alternative design A. Specifically, the total score of the design B matrix (298.78) is much higher than that of design A (147.09). The superiority of the actuator design alternative B is reflected in better performance in all aspects of dorsiflexion-plantar flexion and inversion-eversion movements. More efficient torque parameters, safety factors, and structural deformations are more suitable for meeting the needs of post-stroke ankle rehabilitation.

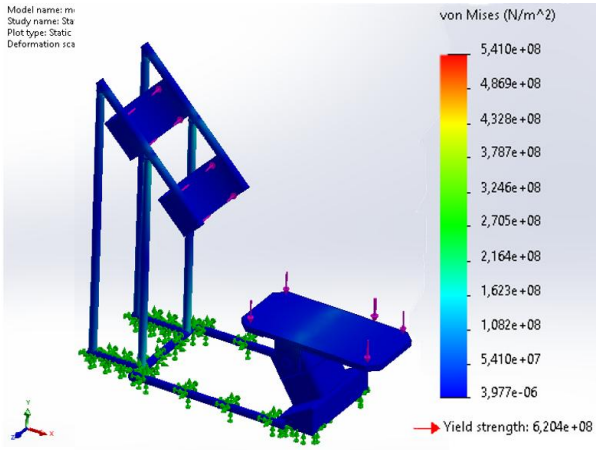

(a)

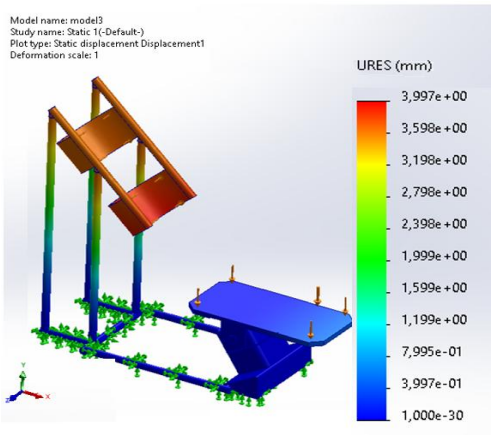

(b)

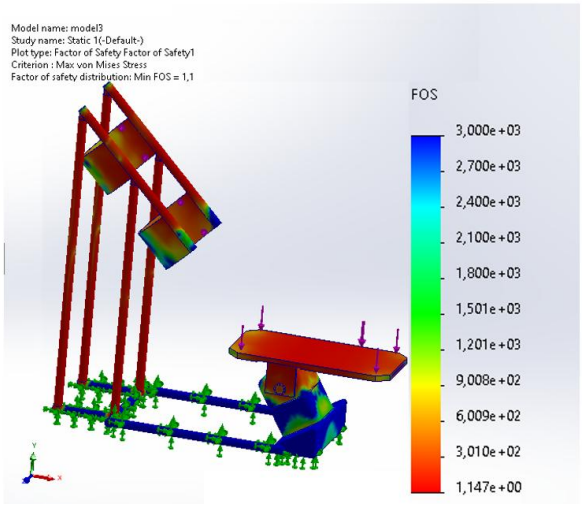

(c)

Figure 10. FEA simulation results on exoskeleton design alternative B (a) Tension test, (b) Displacement test, (c) Safety factor

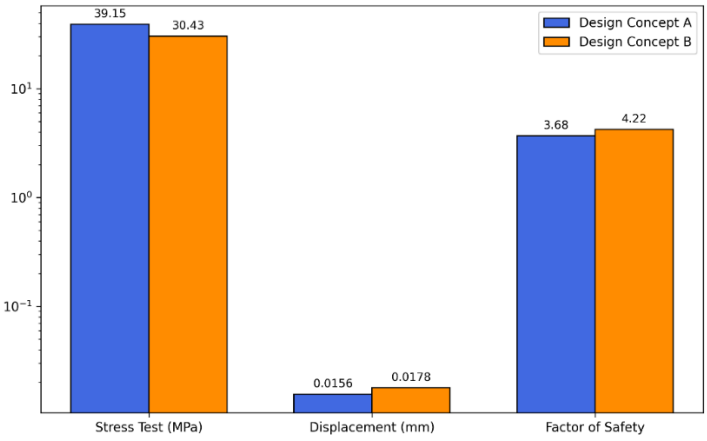

Figure 11. Recapitulation of the FEA simulation between alternative design A and design B

One important factor that is of concern is the torque value generated in each design alternative. Design alternative B is supported by the placement of the rotation actuator structure higher and parallel to the calf leg support section, making the center axis of the foot and the vertical structure closer together. This configuration enables more efficient force transfer and reduces unwanted torsional moments. Design alternative B is confirmed based on lower dorsiflexion-plantarflexion and inversion-eversion torque values compared to design alternative A. Design B demonstrates precision and mechanical efficiency, making it more efficient in terms of energy use, load distribution, and the effectiveness of ankle rotation actuation control, which is crucial in supporting optimal ankle rehabilitation.

Table 5. Decision evaluation matrix with weight values on two exoskeleton design alternatives

Evaluation Criteria	Importance Factor	Concept A Performance	Calculated Score A	Concept B Performance	Calculated Score B
Inversion-eversion Torque (N.m.)	25%	170	33.5	134	42.5
Dorsi flexion-plantar flexion Torque (N.m.)	30%	842	108.6	360	252
Safety Factor	25%	3.68	0.92	4.22	1.055
Tensile Test (MPa)	10%	39.15	3.915	30.43	3.043
Displacement (mm)	10%	1.55	0.155	1.78	0.178
Total	100%		147.09		298.78

4. CONCLUSIONS

The exoskeleton concept described in this study serves as a design guide for ankle rehabilitation devices targeting individuals with post-stroke conditions. The development process considers physiological, biomechanical, and technical issues related to the patient's pathological conditions to provide thorough design requirements. Anthropometric and physiological evaluations of the ankle joint inform important design factors, including structural performance and material choices. The resultant exoskeleton design is tailored to human ankle measurements, ensuring ergonomic compatibility and minimizing the risk of mechanical interference with artificial components. Mechanical evaluation to ensure compatibility with the computer-aided design specifications, which establish the foundational mechanical parameters necessary for production. Both kinetic and stationary assessments form integral components of this engineering approach. Subsequently, material evaluation procedures are implemented through structural stress examination, incorporating a blend of materials including polylactic acid, polyvinyl chloride, and aluminum alloys, which are specifically selected to complement the two proposed exoskeleton configurations. A comparative study across several performance indicators reveals that the B design configuration outperforms the first by offering an ideal balance of safety factor margins, structural torque, displacement, and stress tests. Exhibiting an enhanced protective coefficient of 4.22, reduced structural stress levels at 30.43 MPa, and decreased rotational requirements of 360 N-m and 134 N-m. This configuration not only delivers improved safety parameters and load distribution capabilities but also demonstrates greater operational efficiency in terms of power consumption and activation mechanisms. While experiencing marginally increased deformation values, this minor limitation does not compromise the comprehensive benefits offered by the B design, establishing it as a more effective and dependable solution compared to the initial configuration.

ACKNOWLEDGEMENTS

The authors would like to express their sincere gratitude to the Institute for Research and Community Service (LPPM) at Bojonegoro University for the financial support provided under grant number [053/LPPM-LIT/UB/IV/2024]. This support has been essential in facilitating the research activities and the successful completion of this research

CONFLICT OF INTEREST

The author declares that the research results in this manuscript do not contain any financial, personal, or professional conflicts of interest that could give rise to activities that could be considered as potential conflicts of interest.

AUTHORS' CONTRIBUTIONS

E. W. Abryandoko (Conceptualization; methodology; CAD modeling; FEA analysis; writing original draft preparation)

F. Ashari (Supervision; validation; critical review; and editing of the manuscript)

AVAILABILITY OF DATA AND MATERIALS

All data generated or analyzed during this research are included in this published article and its supplementary files. Additional datasets are available from the corresponding author upon reasonable request.

ETHICS STATEMENT

This research did not involve human participants or animals. All procedures were based on computer-aided design (CAD) modeling, motion analysis, and finite element simulations, which do not require ethical approval.

REFERENCES

[1] V. L. Feigin, G. A. Roth, M. Naghavi, P. Avan, C. Barker, E. Brainin, et al., "World stroke organization (WSO): Global stroke fact sheet 2022," *International Journal of Stroke*, vol. 17, no. 1, pp. 18-29, 2022.

[2] A. K. Boehme, C. Esenwa, M. S. V. Elkind, "Stroke risk factors, genetics, and prevention," Circulation Research, vol. 120, no. 3, pp. 472-495, 2017.

[3] W. J. Tu, S. J. Wang, S. Yin, X. Xu, R. Y. Zheng, L. L. Zeng, et al., "China stroke surveillance report 2021," *Military Medical Research*, vol. 10, no. 1, p. 33, 2023.

[4] U. B. Flansbjer, A. M. Holmbäck, D. Downham, C. Patten, J. Lexell, "Reliability of gait performance tests in men and women with hemiparesis after stroke," *Journal of Rehabilitation Medicine*, vol. 37, no. 2, pp. 75-82, 2005.

[5] J. Hayakawa, S. Ohtsuka, R. Hashimoto, T. Kanai, T. Wakasa, M. Tsukagoshi, "Reliability of and minimal detectable changes in gait performance tests in patients with chronic hemiplegic stroke," *Journal of Stroke Medicine*, vol. 3, no. 1, pp. 34-39, 2020.

[6] A. Bourgeois, B. Rice, C. H. Goh, "Design optimization of the lift mechanism in the robotic walking training device using the engineering design methodology," *Applied Sciences*, vol. 14, no. 1, p. 327, 2024.

[7] A. Roy, H. I. Krebs, D. J. Williams, C. T. Bever, L. W. Forrester, R. F. Macko, et al., "Robot-aided neurorehabilitation: A novel robot for ankle rehabilitation," *IEEE Transactions on Robotics*, vol. 25, no. 3, pp. 569-582, 2009.

[8] M. Shi, C. Yang, D. Zhang, "A novel human-machine collaboration model of an ankle joint rehabilitation robot driven by EEG signals," *Mathematical Problems in Engineering*, vol. 2021, p. 5564235, 2021.

[9] Q. Meng, G. Liu, X. Xu, Q. Meng, H. Yu, "Design and analysis of a supine ankle rehabilitation robot for early stroke recovery," *Machines*, vol. 11, no. 8, p. 787, 2023.

[10] J. Li, K. Yang, D. Yang, "Wearable ankle assistance robot for a human walking with different loads," *Mechanical Sciences*, vol. 14, no. 2, pp. 429-438, 2023.

[11] J. Bessler, A. L. Prange-Lasonder, R. Schaake, J. H. Buurke, G. B. Rietman, A. Melendez-Calderon, "Safety assessment of rehabilitation robots: A review identifying safety skills and current knowledge gaps," *Frontiers in Robotics and AI*, vol. 8, p. 602878, 2021.

[12] A. Giallanza, G. La Scalia, R. Micale, C. M. La Fata, "Occupational health and safety issues in human-robot collaboration: State of the art and open challenges," *Safety Science*, vol. 169, p. 106313, 2024.

[13] R. Barkataki, Z. Kalita, S. Kirtania, "Anthropomorphic design and control of a polycentric knee exoskeleton for improved lower limb assistance," *Intelligent Service Robotics*, vol. 17, no. 3, pp. 555-577, 2024.

[14] R. S. Gonçalves, L. A. O. Rodrigues, R. Humbert, G. Carbone, "A user-friendly nonmotorized device for ankle rehabilitation," *Robotics*, vol. 12, no. 2, p. 32, 2023.

[15] J. Narayan, S. Kumar Dwivedy, "Preliminary design and development of a low-cost lower-limb exoskeleton system for paediatric rehabilitation," *Proceedings of the Institution of Mechanical Engineers Part H Journal of Engineering in Medicine*, vol. 235, no. 5, pp. 530-545, 2021.

[16] S. H. Collins, M. Bruce Wiggin, G. S. Sawicki, "Reducing the energy cost of human walking using an unpowered exoskeleton," *Nature*, vol. 522, no. 7555, pp. 212-215, 2015.

[17] A. Bourgeois, B. Rice, C. H. Goh, "Design optimization of the lift mechanism in the robotic walking training device using the engineering design methodology," *Applied Sciences*, vol. 14, no. 1, p. 327, 2024.

[18] C. L. Brockett, G. J. Chapman, "Biomechanics of the ankle," *Orthopaedics and Trauma*, vol. 30, no. 3, pp. 232-238, 2016.

[19] R. K. Salih, W. S. Aboud, "Smart robotic exoskeleton: Constructing using 3D printer technique for ankle-foot rehabilitation," *Journal of Robotics and Control*, vol. 4, no. 4, pp. 537-547, 2023.

[20] J. M. Medina McKeon, M. C. Hoch, "The ankle-joint complex: A kinesiologic approach to lateral ankle sprains," *Journal of Athletic Training*, vol. 54, no. 6, pp. 589-602, 2019.

[21] Z. Nursultan, C. Marco, G. Balbayev, "A portable robotic system for ankle joint rehabilitation," *Electronics*, vol. 12, no. 20, p. 4271, 2023.

[22] C. Alves, A. Whiteley, C. Jennings, L. Murphy, J. Walsh, A. Burns, et al., "Plantar flexion, dorsiflexion, range of movement and hindfoot deviation are important determinants of foot function in children," *Journal of Children's Orthopaedics*, vol. 13, no. 5, pp. 486-499, 2019.

[23] S. Nagarajan, K. Mohanavelu, S. Sujatha, "A simulation-based framework to determine the kinematic compatibility of an augmentative exoskeleton during walking," *Robotics*, vol. 13, no. 5, p. 79, 2024.

[24] M. D. C. Sanchez-Villamañan, J. Gonzalez-Vargas, D. Torricelli, J. C. Moreno, J. L. Pons, "Compliant lower limb exoskeletons: A comprehensive review on mechanical design principles," *Journal of NeuroEngineering and Rehabilitation*, vol. 16, no. 1, p. 55, 2019.

[25] E. W. Abryandoko, S. Susmartini, P. W. Laksono, L. Herdiman, "Simulation and modeling of hybrid assistive robotic neuromuscular dynamic stimulation for upper limb rehabilitation," *Journal of Applied Science and Engineering*, vol. 28, no. 5, pp. 925-933, 2025.

[26] H. Ren, T. Liu, J. Wang, "Design and analysis of an upper limb rehabilitation robot based on multimodal control," *Sensors*, vol. 23, no. 21, p. 8801, 2023.

[27] B. Li, B. Yuan, J. Chen, Y. Zuo, Y. Yang, "Mechanical design and human-machine coupling dynamic analysis of a lower extremity exoskeleton," in *Lecture Notes in Computer Science*, vol. 10462, pp. 593-604, 2017.

[28] G. Sergazin, K. Kappassov, A. Adiyatov, A. Massalin, A. Varol, H. A. Varol, "Design, simulation and functional testing of a novel ankle exoskeleton with 3DOFs," *Sensors*, vol. 24, no. 19, p. 6160, 2024.

[29] S. Grazioso, T. Caporaso, and G. Di Gironimo, "Decision support in engineering design: The ELIGERE open source software platform," International Journal on Interactive Design and Manufacturing, vol. 18, no. 1, pp. 509-524, 2024.

[30] B. Zhang, M. Ma, Z. Wang, "Promoting active aging through assistive product design innovation: A preference-based integrated design framework," *Frontiers in Public Health*, vol. 11, p. 1203830, 2023.

[31] S. Głowiński, T. Krzyżyński, S. Pecolt, I. Maciejewski, "Design of motion trajectory of an arm exoskeleton," *Archive of Applied Mechanics*, vol. 85, no. 1, pp. 75-87, 2015.

[32] L. Zhang, Y. Liu, R. Wang, C. Smith, E. M. Gutierrez-Farewik, "Modeling and simulation of a human knee exoskeleton's assistive strategies and interaction," *Frontiers in Neurorobotics*, vol. 15, p. 620928, 2021.

[33] S. Śpiewak, T. Gzik-Zroska, D. Gzik, K. Joszko, S. Wolański, M. Gzik, et al., "Modeling and strength calculations of parts made using 3D printing technology and mounted in a custom-made lower limb exoskeleton," *Materials*, vol. 17, no. 14, p. 3406, 2024.

[34] L. Sha, A. Lin, X. Zhao, S. Kuang, "A topology optimization method of robot lightweight design based on the finite element model of assembly and its applications," *Science Progress*, vol. 103, no. 3, pp. 1-16, 2020.

[35] N. A. Bianco, S. H. Collins, K. Liu, S. L. Delp, "Simulating the effect of ankle plantarflexion and inversion-eversion exoskeleton torques on center of mass kinematics during walking," *PLoS Computational Biology*, vol. 19, no. 8, p. e1010712, 2023.

[36] A. Rojas, J. Ronceros, C. Raymundo, G. Zapata, L. Vinces, G. Ronceros, "Numerical simulation and design of a mechanical structure of an ankle exoskeleton for elderly people," *Technologies*, vol. 12, no. 7, p. 107, 2024.

[37] M. Cempini, S. M. M. De Rossi, T. Lenzi, N. Vitiello, M. C. Carrozza, "Self-alignment mechanisms for assistive wearable robots: A kinetostatic compatibility method," *IEEE Transactions on Robotics*, vol. 29, no. 1, pp. 236-250, 2013.

[38] M. O. Ajayi, K. Djouani, Y. Hamam, "Interaction control for human-exoskeletons," *Complexity*, vol. 2020, p. 8472510, 2020.

[39] G. M. Achilli, G. Logozzo, M. C. Valigi, S. Strainovic, A. Coppa, C. Canali, et al., "Soft, rigid, and hybrid robotic exoskeletons for hand rehabilitation: Roadmap with impairment-oriented rationale for devices design and selection," *Applied Sciences*, vol. 13, no. 20, p. 11287, 2023.

[40] M. M. Rodgers, G. Alon, V. M. Pai, R. S. Conroy, "Wearable technologies for active living and rehabilitation: Current research challenges and future opportunities," *Journal of Rehabilitation and Assistive Technologies Engineering*, vol. 6, pp. 1-9, 2019.

[41] G. Kwakkel, J. Collier, J. M. Veerbeek, P. Nene, B. Jurcovicova, B. Molad, et al., "Motor rehabilitation after stroke: European stroke organisation (ESO) consensus-based definition and guiding framework," *European Stroke Journal*, vol. 8, no. 4, pp. 851-868, 2023.

[42] M. F. Hamza, R. A. R. Ghazilla, B. B. Muhammad, H. J. Yap, "Balance and stability issues in lower extremity exoskeletons: A systematic review," *Biocybernetics and Biomedical Engineering*, vol. 40, no. 4, pp. 1666-1685, 2020.

[43] T. Wang, B. Peng, B. Zhang, T. Duan, W. Wei, M. O. Tokhi, et al., "A review on the rehabilitation exoskeletons for the lower limbs of the elderly and the disabled," *Electronics*, vol. 11, no. 3, p. 388, 2022.

[44] S. K. Hasan, A. K. Dhingra, "Performance verification of different control schemes in human lower extremity rehabilitation robot," *Results in Control and Optimization*, vol. 4, p. 100028, 2021.

[45] R. Rituraj, R. Scheidl, P. Ladner, M. Lauber, A. Plöckinger, "Prototyping and experimental investigation of digital hydraulically driven knee exoskeleton," *Energies*, vol. 15, no. 22, p. 8695, 2022.

[46] R. Rituraj, R. Scheidl, P. Ladner, M. Lauber, A. Plöckinger, "Prototyping and experimental investigation of digital hydraulically driven knee exoskeleton," *Energies*, vol. 15, no. 22, p. 8695, 2022.

[47] M. Paterna, C. De Benedictis, C. Ferraresi, "Preliminary testing of a passive exoskeleton prototype based on McKibben muscles," *Machines*, vol. 12, no. 6, p. 388, 2024.

[48] Z. Zhu, L. Liu, W. Zhang, C. Jiang, X. Wang, J. Li, "Design and motion control of exoskeleton robot for paralyzed lower limb rehabilitation," *Frontiers in Neuroscience*, vol. 18, pp. 1-19, 2024.

[49] P. Falkowski, K. Jeznach, "Simulation of a control method for active kinesiotherapy with an upper extremity rehabilitation exoskeleton without force sensor," *Journal of NeuroEngineering and Rehabilitation*, vol. 21, no. 1, p. 67, 2024.

[50] A. KhalilianMotamed Bonab, D. Chiaradia, A. Frisoli, and D. Leonardis, "A framework for modeling, optimization, and musculoskeletal simulation of an elbow–wrist exosuit," *Robotics*, vol. 13, no. 4, p. 60, 2024.

[51] I. Ben Abdallah, Y. Bouteraa, "An optimized stimulation control system for upper limb exoskeleton robot-assisted rehabilitation using a fuzzy logic-based pain detection approach," *Sensors*, vol. 24, no. 4, p. 1047, 2024.

[52] K. Kiguchi, M. H. Rahman, M. Sasaki, K. Teramoto, "Development of a 3DOF mobile exoskeleton robot for human upper-limb motion assist," *Robotics and Autonomous Systems*, vol. 56, no. 8, pp. 678-691, 2008.

[53] G. Mashud, S. K. Hasan, N. Alam, "Advances in control techniques for rehabilitation exoskeleton robots: A systematic review," *Actuators*, vol. 14, no. 3, p. 108, 2025.

[54] J. Li, Y. Tai, F. Meng, "Rehabilitation exoskeleton torque control based on PSO-RBFNN optimization," *PLoS One*, vol. 18, no. 8, p. e0285453, 2023.